THE USE OF ENERGY METHODS AT THE CALCULATION OF VEHICLE IMPACT VELOCITY

ANDRZEJ ŻUCHOWSKI[1]

Military University of Technology

Summary

The relations between the deformation of the front crumple zone of a motor car and the velocity of a car impact against a barrier have been explored. To determine the parameters of the energy models employed at the vehicle collision analysis, results of 18 crash tests carried out with three motor car models were used. The crash tests represented frontal impacts of the cars against a barrier with velocities of 40 km/h, 48 km/h, and 56 km/h. The values obtained for the energy model parameters were considered in relation to the values given in the literature. The attention was focussed on the linear models that are used in the simplified, Campbell, and McHenry methods, with evaluating the effectiveness of such models when applied to present-day cars. The methods are based on the dimensions of deformation of the crumple zone. It was found that the method of determining the vehicle deformation caused by the impact against an obstacle could affect the results of calculation of the impact velocity. The relations between the velocity of impact against a barrier and the deformation of the front crumple zone of motor vehicles of various categories have been presented, based on results of several hundred crash tests. It has been indicated that the characteristics of the front crumple zone in present-day cars differ from those of the cars manufactured 20 to 30 years ago. Therefore, the changes having been introduced to motor vehicle construction must be taken into account when the values of the parameters used in the energy methods are determined.

Keywords: frontal impact, road accident reconstruction, energy methods, bodywork deformation

1. Introduction

The determining of the initial velocity of a motor vehicle in the pre-impact phase is often a matter of critical importance in the process of reconstruction of a road accident. The use of data obtained from motor vehicle "black boxes" (such as *Accident Data Recorder, Event Data Recorder*, or *Unfall Daten Speicher*) for this purpose will considerably facilitate this task in the future. Nevertheless, the calculation methods are still in use at present, where the relations between the vehicle velocity at the very beginning of the bodywork deformation process and the energy required to cause the deformation are taken into account. Such relations are described with the use of energy methods, where mathematical "energy

---

[1] Military University of Technology, Faculty of Mechanical Engineering, ul. Gen. S. Kaliskiego 2, 00-908 Warszawa, Poland, e mail: azuchowski@wat.edu.pl, tel. +48 22 261 837 454

models" are employed. An important problem inherent in the use of the energy models arises from limited availability of the values of parameters of such models that would adequately represent present-day motor vehicles, while the use of incorrect data for the calculations may result in erroneous estimation of the impact velocity and, in consequence, in the issuing of an incorrect opinion.

The energy methods employed at the reconstruction of road accidents are based on measurements of the vehicle deformation that has arisen from the vehicle impact against an obstacle. The size of such a deformation depends on the impact velocity, stiffness of the vehicle structure at the place where it came into contact with the obstacle, and characteristics of the obstacle. Other factors of significant importance include the vehicle mass as well as the bodywork construction, which undergoes various improvements in successive vehicle generations [14]. Car frontal stiffness depends not only on the bodywork construction but also on the arrangement of components of the power transmission system and engine auxiliaries in the engine compartment.

The objective of this work was to assess the results of calculations of the pre-impact velocity of a vehicle, where the calculations were carried out with the use of energy methods and an assumption of a linear relation between the vehicle velocity (or the force crushing the bodywork) and the deformation of the bodywork structure. A description and examples of application the energy methods have been given in many publications, e.g. [1, 2, 4, 5, 6, 7, 10, 11, 18, 20, 24]. This analysis covers a simplified method and the Campbell and McHenry methods, employed *inter alia* in the PC Crash program.

In this work, attention was focused on the frontal impact of a motor car against an obstacle. The effectiveness of the energy methods was evaluated by comparing the known value of the velocity of a car impact against a rigid barrier with the velocity value determined with the use of energy methods. Answers were sought to the questions whether changes in vehicle construction had considerably affected the values of the parameters used in the energy methods and which of the methods under analysis would give the best results.

Based on the crash test results published on the Internet by the *National Highway Traffic Safety Administration* (NHTSA) [26], relations between the velocity of impact against a barrier and the deformation of the front crumple zone have been presented for several hundred motor vehicles of various categories. Crash test results obtained for three car models were analysed in detail, with special attention being paid to the description of the deformations and to the stiffness characteristics of the front crumple zone. The experiment and calculation results were used for defining the parameters of the energy models for the three cars and they were compared with the data available from the literature, with highlighting the scatter of the measurement results obtained from crash tests carried out in the same test conditions.

2. Objects of the investigation

The relations between the velocity of impact against a barrier and the deformation of the front crumple zone of the cars were evaluated on the grounds of results of testing three

car models. The cars were selected for the analysis according to the following criteria:

– the crash test was to represent an impact against a rigid barrier situated perpendicularly to the direction of vehicle motion;
– the vehicles subjected to the crash tests had to represent different market sectors (car categories) and they years of manufacture were not to differ from each other too much;
– the crash tests of each specific car model should have been carried out at three impact velocity values, equal to 40 km/h, 48 km/h, and 56 km/h;
– at least two crash tests of the same car model should have been carried out at a specific value of the velocity of impact against a barrier.

Much attention was paid to the vehicle identification, which was aimed at determining the degree of similarity of individual specimens of a specific car model. The similarity was defined with taking into account the following factors: vehicle body type, year of manufacture, engine cubic capacity and position (transverse or longitudinal), gearbox type (manual or automatic), drive axle (front or rear), mass, dimensions (including tyre size), and vehicle identification number (VIN). An important part of the vehicle similarity assessment was the comparison of bodywork stiffness curves, dealt with in Section 4 (Fig. 5). Photographs of the car models subjected to the analysis have been shown in Fig. 1. In total, results of 18 crash tests were analysed. The general vehicle characteristics have been presented in Table 1. The Honda Accord cars differed from each other in the gearbox type (manual and automatic) and the Ford Escape car versions were either front-wheel drive or four-wheel drive.

Fig. 1. The cars subjected to the analysis [26]

Table 1. Car characteristics (based on [26])

Make, model, year, body type	Powertrain	Mass [kg]	Length [m]	Width [m]	Tyre size
Toyota Echo, 2001, sedan	Engine 1.5 dm^3, 4-cylinder in line, transverse, front-wheel drive, automatic gearbox	1099 – 1158	4.13	1.66	P175/65/R14
Honda Accord, 2001, sedan	Engine 2.3 dm^3, 4-cylinder in line, transverse, front-wheel drive, automatic or manual gearbox	1500 – 1597	4.78	1.78	P195/65/R15
Ford Escape, 2001, SUV	Engine 3 dm^3, V6, transverse, front-wheel drive or 4WD, automatic gearbox	1733 – 1797	4.36	1.74	P235/70/R16

3. Analysis of results of car deformation measurements

For the vehicle deformation resulting from a crash test to be determined, the vehicle body dimensions are usually measured before and after the collision with the barrier. Fig. 2 shows the car deformation dimensions defined by distances C_1, C_2, ..., C_6, which are measured at points evenly distributed along line segment L; the length L is usually shorter than the vehicle width S. The dimension $C*$ refers to the deformation depth measured at the height of the bumper, at the midpoint of bumper length (in the longitudinal symmetry plane of the car).

The results of car deformation measurements at three values of the velocity of impact against a barrier have been shown in Fig. 3. The original contour of the car body has been represented by the lines denoted as "BEFORE". The fine black lines represent the bodywork deformations at individual crash tests (two tests at each test velocity). The deformation depth values at some points differed from each other quite largely; anyway, the differences do not exceed 6–7 cm. For each pair of tests carried out at a specific impact velocity, averaged deformation lines were plotted and denoted in the graphs with the corresponding impact velocity value.
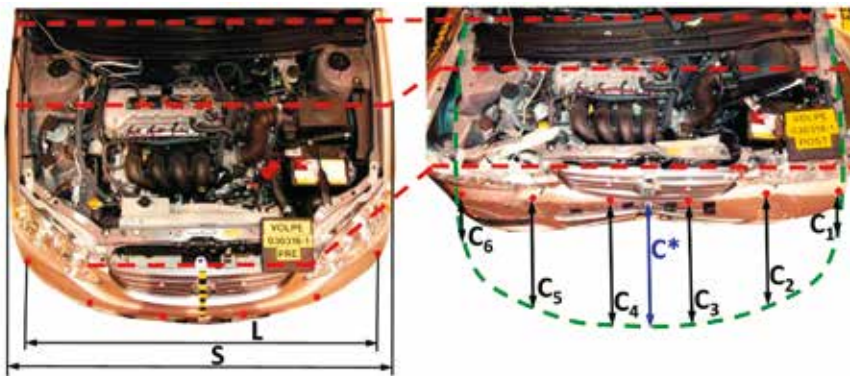
Fig. 2. Car deformation after an impact against a rigid barrier (photographs published in [26])

Interestingly, the crumple zone of a car having hit a rigid flat barrier was not evenly deformed over the whole vehicle width. This was an effect of elastic interactions between the vehicle components present in the engine compartment and parts of the vehicle body. As an example, the central part of the crumple zone of the Ford Escape was much more deformed than its side areas at the impact velocity of 56 km/h. In this case, this could result from the fact that the vehicle wheels counteracted the deformation of the front body panel. In the Honda Accord at the impact velocity of 56 km/h, the deformations at places corresponding to dimensions C_2 and C_5 markedly exceeded those observed at the other places. This may be explained as follows: the places C_1, C_3, C_4, and C_6 could be deformed during the contact with the barrier similarly to the places C_2 and C_5, but when the car bounced off the barrier, they could be pushed back (i.e. to the vehicle front) due
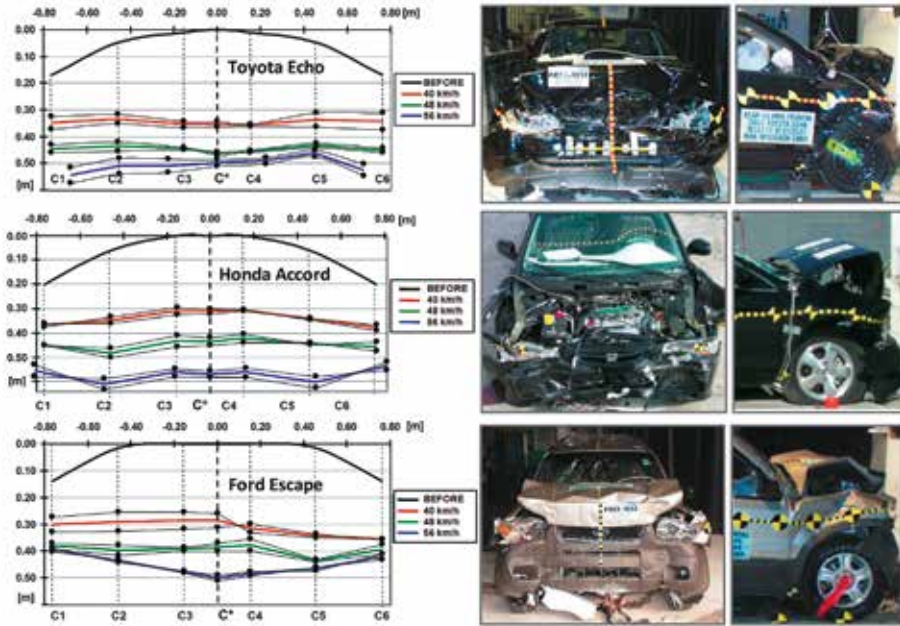
Fig. 3. Deformations of cars Toyota Echo, Honda Accord, and Ford Escape
(the photographs show the cars after the impact against a barrier with a velocity of 56 km/h [26])

to the elastic strains present in the structure. The deformations of the Toyota Echo at the impact velocity of 56 km/h were deeper on the left vehicle side (at places C_1, C_2, and C_3). This effect could result from different stiffness of the crumple zone on the left and right side of the engine compartment, which may sometimes cause the vehicle to rotate by a small angle during a perpendicular impact against a flat barrier [12].

If linear energy models are to be used, the deformation assumed for the calculations must be expressed by a single number. However, a fundamental problem arises here, how a single number can represent the three-dimensional vehicle deformation. In practice, the size of vehicle deformation, especially in the case of partial deformation (i.e. when the deformation does not extend over the whole vehicle width), may be defined by the "average deformation" (denoted here by "$C_{śr}$"[2]), calculated from dimensions C_1, ..., C_6 [10, 11, 21, 22]:

$$C_{śr} = \frac{1}{5}\left(\frac{C_1}{2} + C_2 + C_3 + C_4 + C_5 + \frac{C_6}{2}\right) \tag{1}$$

For the description of the deformation of a vehicle that has frontally hit a rigid flat barrier, the use of the deformation parameter C^* previously mentioned or the maximum deformation C_{max} may be considered, with the latter being defined as the distance between two vertical planes perpendicular to the longitudinal symmetry plane of the vehicle, such that one of

---

[2] The subscript "$_{śr}$", wherever used in this paper, indicates the average value. *Translator's note.*

them goes through the most forwards point of the vehicle body before the impact against a barrier and the other one goes through the most deeply displaced point of the front vehicle surface having been deformed. Should the projection of the deformed area on the ground plane be approximated by a shape close to a rectangle then an expression $C_{śr} \approx C^* \approx C_{max}$ would hold. The C_{max} deformation value has no practical application to the reconstruction of road accidents but it has been mentioned here to show the relation between the plastic deformation (also referred to as static or permanent deformation) and the dynamic deformation described in the subsequent part of this paper.

Based on the averaged vehicle deformation lines, the deformation values C_{max}, C^*, and $C_{śr}$ were calculated. The calculation results have been brought together in Table 2. The following relations can be formulated on these grounds:

$$C_{śr} = (0,81...0,97) \cdot C^* \text{ and } C_{max} = (1,00...1,24) \cdot C^* \tag{2}$$

Table 2. Vehicle deformation vs. velocity of vehicle impact against a barrier

Vehicle	V [km/h]	C_{max} [m]	C^* [m]	$C_{śr}$ [m]	L [m]	S [m]
Toyota Echo	56	0.564	0.498	0.446	1.347	1.66
	48	0.463	0.463	0.386	1.525	
	40	0.357	0.354	0.288		
Honda Accord	56	0.610	0.569	0.506	1.636	1.78
	48	0.481	0.434	0.381	1.525	
	40	0.377	0.311	0.270		
Ford Escape	56	0.500	0.500	0.420	1.515	1.74
	48	0.436	0.385	0.364	1.525	
	40	0.356	0.286	0.278		

Table 2 also includes the values of vehicle width S and length of line segment L (averaged out of two measurements), which is defined as the distance between the outermost points of the area for which the deformations C_1, ..., C_6 are measured (cf. Fig. 2). The distance L makes here 81–92% of the width of the vehicles under consideration and has been described in test reports [26] (as well as in the PC Crash program, method CRASH3) as the vehicle body deformation width, which arouses doubts. In fact, we have $L = 1.525$ m for every car under consideration when tested at impact velocities of 40 km/h and 48 km/h, regardless of the actual vehicle width (the tests were carried out at the same laboratory). For the Toyota Echo and Ford Escape cars, the length L measured at the impact velocity of 56 km/h (at other test laboratories) was shorter than that measured at the velocities of 40 km/h and 48 km/h. Moreover, the locations of the places of measurement of deformations C_1, ..., C_6 were defined in different ways at the tests of different cars, e.g. for the testing of the Toyota Echo cars at impact velocities of 40 km/h and 48 km/h, the distance between the points of measurement of deformations C_1 and C_6 was divided into 5 equal parts while it was divided into 6 equal parts when the impact velocity was 56 km/h (cf. Fig. 3). In consideration of the doubts whether the distance L correctly represents the

deformation width, the analysis was further carried out with assuming L as equal to the vehicle width S.

The relations between $C_{śr}$ and C^* were defined on the grounds of results of testing 448 cars at impact velocities of 48 km/h and 56 km/h [26]. The vehicles were categorized in accordance with the American classification, which was also used in handbook [11]. The categorization covered motor cars with coupe, sedan, hatchback, estate car, and van body versions (the pickups and SUVs were omitted). Table 3 shows the mass and dimension characteristics of cars classified under specific categories and the relations between $C_{śr}$ and C^*. The reciprocally corresponding $C_{śr}$ and C^* values determined for cars of individual categories have been compared with each other in the graphs in Fig. 4.

Table 3. Relations between the $C_{śr}$ and C^* deformation values for cars of various categories (tests at impact velocities of 48 km/h and 56 km/h)

Category	Number of cars tested	Mass [kg]	Wheelbase [m]	Length [m]	Width [m]	Car model years 1974–1989	Car model years 1994–2013
Mini (M)	53	900,,,1180	2.14...2.54	3.50...4.43	1.34...1.70	$C_{śr}$=(0.84... 1.01)·C^*	$C_{śr}$=(0.82... 0.99)·C^*
Subcompact (S)	96	1260...1450	2.32...2.67	3.94...4.08	1.67...1.80	$C_{śr}$=(0.83... 1.01)·C^*	$C_{śr}$=(0.78... 0.98)·C^*
Compact (C)	148	1480...1730	2.62...2.81	4.70...5.15	1.75...1.88	$C_{śr}$=(0.87... 1.01)·C^*	$C_{śr}$=(0.74... 0.97)·C^*
Intermediate (I)	111	1800...2200	2.79...3.08	4.83...5.51	1.80...1.90	$C_{śr}$=(0.91... 0.99)·C^*	$C_{śr}$=(0.76... 0.99)·C^*
Van (V)	40	1780...2270	2.46...3.18	4.43...5.18	1.74...2.01	$C_{śr}$=(0.88... 1.00)·C^*	$C_{śr}$=(0.80... 0.96)·C^*

For car model years 1974–1989, we can observe markedly smaller differences between the $C_{śr}$ and C^* values (cf. the distances between individual points and the "1:1" line). This may be caused by different shape of the contour of the front part of the vehicle body, more resembling a rectangle in the older car designs. Another important finding can be seen in Fig. 4: the deformation values observed for present-day cars are markedly lower in than those recorded for car model years 1974–1989 (especially for cars classified under the subcompact, compact, and intermediate categories). More information about the relations between the deformation of the cars tested and their mass and year of manufacture can be found in publication [14].
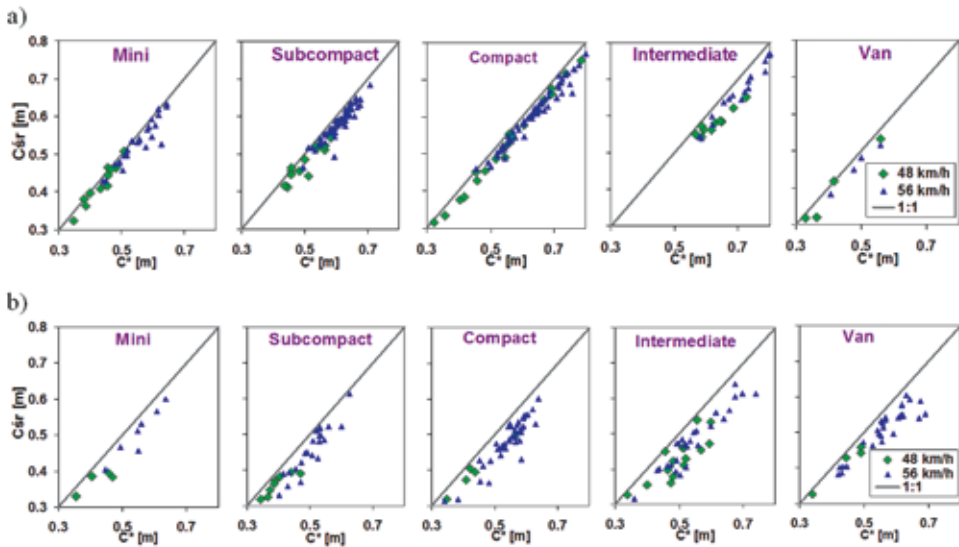
Fig. 4. Relations between the $C_{śr}$ and C^* deformation values for cars of various categories
(tests at impact velocities of 48 km/h and 56 km/h):
a) car model years 1974–1989 (n = 230); b) car model years 1994–2013 (n = 218)

4. Analysis of vehicle stiffness characteristics

Important information about the course of the vehicle collision process is provided by the characteristic curve representing the stiffness of the front crumple zone. The curve shows changes in the vehicle body crushing force as a function of the total bodywork deformation, i.e. the plastic and elastic deformation, hereinafter referred to as *dynamic deformation* (D). In most cases, the bodywork stiffness curve is plotted on the grounds of the vehicle acceleration recorded during an impact of the vehicle against a flat rigid barrier. The method of determining such a curve has been described in publications [15, 25]. The body crushing force can also be measured with the use of sensors installed in the barrier [5, 12, 13, 25]. The bodywork stiffness curves presented in Fig. 5 were prepared on the grounds of specific realizations of vehicle acceleration during an impact. The vehicle acceleration was measured at several points and the acceleration vs. time curve taken as an input for the calculations was obtained by averaging individual acceleration records. The acceleration records were subjected to centring and filtering, which were important elements of the processing of the measurement results because they could affect the profiles of the bodywork stiffness curves being prepared. For the filtration, a CFC60 filter was used.

Two crash tests of each vehicle model, carried out at specific velocities of vehicle impact against a barrier, were taken into account at the analysis and the bodywork stiffness curves obtained showed significant similarity, although the Honda Acord and Ford Escape

cars used as specimens at the crash tests differed from each other in the construction of the powertrain (see Table 1). Noteworthy is the fact that during the impact, the vehicle accelerations were actually recorded by the measuring system at the places where the sensors were installed. Therefore, instantaneous changes in the acceleration records may be explained by local vibrations of the bodywork structure. As an example, a negative value of the force was reflected in the bodywork stiffness curve of the Toyota Echo at a deformation value of about 0.2 m, at the test with an impact velocity of 40 km/h.
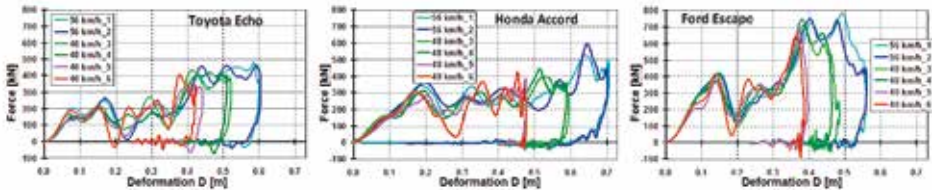
Fig. 5. Bodywork stiffness curves recorded for the Toyota Echo, Honda Accord, and Ford Escape cars

The Toyota Echo and Ford Escape bodywork stiffness curves are characterized by fast growth in the crushing force at a deformation exceeding as small a value as 0.3 m. In Honda Accord, this only took place at a deformation exceeding about 0.6 m, which confirms the role of differences in the construction of the front crumple zone of these cars.

Below, attention has been drawn to the reasons for differences between the plastic deformation C and the dynamic deformation D. With this end in view, the following characteristic quantities that describe the vehicle motion during the collision and the stiffness of the front crumple zone have been shown in Fig. 6:
- elastic deformation D_0 at the beginning of the vehicle body crushing process;
- elastoplastic deformation D_p that takes place at the instant when the vehicle is separated from the obstacle, i.e. when the vehicle body crushing force is $F_z = 0$ (sometimes this deformation is referred to as "deformation at separation" [19]);
- maximum elastoplastic deformation D_{max};
- line segment $(D_{max} - D_p)$, representing the residual elastic deformation [11].
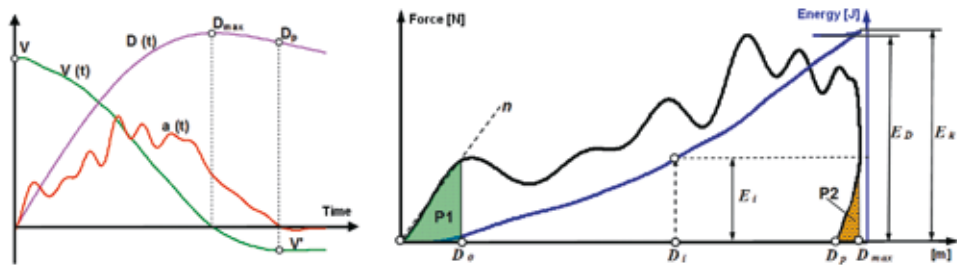
Fig. 6. Characteristic quantities that describe the vehicle motion during the collision and the stiffness of the front crumple zone

In consideration of the fact that that the first part of the bodywork stiffness curve is almost linear (line n in Fig. 6), an assumption was made that displacement D_0 represented the elastic deformation that occurs at a low velocity of impact against a barrier (cf. the b_0 coefficient in the Campbell method described in Section 6). The values of D_0, D_p, and D_{max} were directly read from the bodywork stiffness curve; the D0 value was read from the curve plotted for the impact velocity of 40 km/h, where the beginning of the plastic deformation was best discernible. Table 4 shows a comparison of the dynamic deformation values D_{max} and D_p with the plastic deformation values C_{max} and C^* given in Table 2, with the following indicators having been introduced:

$$\gamma_1 = \frac{D_{max}}{C^*}, \quad \gamma_2 = \frac{D_p}{C^*}, \text{ and } \gamma_3 = \frac{D_p}{C_{max}} \tag{3}$$

Table 4. Comparison between the dynamic and plastic deformations of the car bodies

Vehicle	V [km/h]	D_0 [m]	D_p [m]	D_{max} [m]	γ_1	γ_2	γ_3
Toyota Echo	56	0.06	0.568	0.602	1.21	1.14	1.01
	48		0.490	0.515	1.11	1.06	1.06
	40		0.400	0.432	1.22	1.13	1.12
Honda Accord	56	0.09	0.610	0.704	1.24	1.07	1.00
	48		0.565	0.591	1.36	1.30	1.17
	40		0.469	0.477	1.53	1.51	1.24
Ford Escape	56	0.07	0.520	0.559	1.12	1.04	1.04
	48		0.455	0.475	1.23	1.18	1.04
	40		0.380	0.390	1.36	1.33	1.07

The γ indicator values depict the differences between the dynamic and plastic deformations. The biggest differences were observed for the Honda Accord car, where, as an example, $\gamma_1 = 1.24{-}1.53$. At the impact velocity of 56 km/h, the value of the elastoplastic deformation D_p was close to the C_{max} value for all the cars under consideration. The differences between the dynamic and plastic deformations of cars manufactured in the years 2005–2007 have been described in publication [23].

The relation between the impact velocity and the dynamic deformation can be determined by taking into account the energy dissipated during the collision. The energy corresponding to a given deformation D_i can be calculated from the bodywork stiffness curve according to the following formula:

$$E_i = \int_0^{D_i} F_z \, dD \tag{4}$$

where: F_z – vehicle body crushing force; D – dynamic deformation.

The impact velocity value V_i at which the deformation value D_i occurs is then:

$$V_i = \sqrt{\frac{2E_i}{m}} \tag{5}$$

The results of calculation of the impact velocity value according to (5) have been presented in Fig. 7. They cannot be directly used for the reconstruction of a road accident because the plastic deformation (measured on a post-accident car) and the dynamic deformation (determined from the bodywork stiffness curve) may significantly differ from each other [5, 15, 23], as it has been demonstrated above in Table 4. The results presented in Fig. 7 may be useful when the car is modelled with taking into account the dynamics of the collision process.
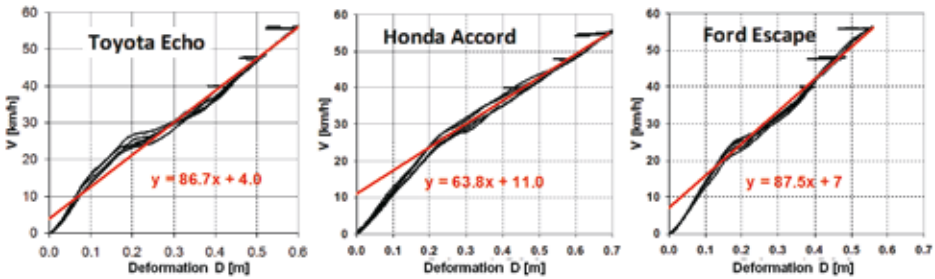
Fig. 7. Relations between the vehicle impact velocity and the dynamic deformation

In Fig. 6, the following areas have also been marked:
- P_1, representing the energy E_0 of elastic deformation of the vehicle body at the beginning of the body crushing process;
- P_2, representing the energy E' of car rebound from the barrier.

The maximum value of integral (4) is equal to the kinetic energy E_k of the car at the instant of hitting the barrier. During the collision, this energy is transformed in its main part into the energy E_p of plastic deformation. After the deformation D_{max} is reached, the energy calculated from equation (4) decreases to a value of ED (Fig. 6). In consideration of the above, the following relations may be formulated, based on the energy balance:

$$E_k = \int_0^{D_{max}} F_z dD = (E_0 + E_P) + E' = E_D + E' \tag{6}$$

$$E_D = E_k - E' = 0{,}5m(V^2 - V'^2) \tag{7}$$

where: m – vehicle mass; V – velocity of the vehicle impact against the barrier; V' – velocity of rebound.

Equation (7) is sometimes expressed in the following form:

$$E_k = E_D + E' = 0{,}5m(V_D^2 - V'^2) \tag{8}$$

and velocity

$$V_D = EES = \sqrt{\frac{2E_D}{m}} \tag{9}$$

is referred to as *Energy Equivalent Speed* (EES) [11]. Noteworthy is the fact that if $V' = 0$ then $V_D = V$ and $E_D = E_k$.

The limiting velocity V_0 at which only the elastic deformation D_0 is present can be calculated in a similar way:

$$V_0 = \sqrt{\frac{2E_0}{m}} \tag{10}$$

A part of the kinetic energy of the vehicle is transformed into the energy of rebound E' as an effect of the residual elastic deformation [11]. The value of the velocity of rebound (V') can be read from the velocity vs. time curve (which can be obtained by integrating the specific realization of vehicle acceleration, cf. Fig. 6) or calculated from the formula

$$V' = \sqrt{\frac{2E'}{m}} \tag{11}$$

The velocity of rebound V' may be expressed with the use of the coefficient of restitution k_{res}. In the case of a motor vehicle collision with a rigid barrier, we have

$$V' = -k_{res} \cdot V \tag{12}$$

The results of calculation of the quantities described above have been brought together in Table 5. As a basic finding, it was ascertained that the energy of deformation E_D made 95.1–99.8% of the kinetic energy E_k and the velocity V_D exceeded 98% of the initial velocity V; this means that an assumption made that $V_D = V$ translates into a calculation error not exceeding 2%. A few important conclusions have been formulated below:

- the values of the velocity V_0 were about 8–11 km/h;
- the values of the velocity of rebound V' of the Toyota Echo and Ford Escape cars fell within limits from 4 km/h to 9 km/h, with the higher values being observed at higher velocities of the vehicle impact against a barrier;
- for the Toyota Echo and Ford Escape cars, the values of the coefficient of restitution fell within limits of 0.090–0.133 and 0.147–0.167, respectively, and they did not depend on the velocity of the vehicle impact against a barrier;
- for the Honda Accord, the values of the coefficient of restitution fell within quite a wide range of 0.046–0.221 and they largely depended on the velocity of the vehicle impact against a barrier (the highest values of this coefficient occurred at the impact velocity of 56 km/h, at which the velocity of rebound was about 11–12 km/h).

Table 5. Tabulated summary of the results of calculation of energy, velocities, and coefficient of restitution

Vehicle	V [km/h]	$Mass$ [kg]	E_k [kJ]	E_0 [kJ]	V_0 [km/h]	E_D [kJ]	V_D [km/h]	E' [kJ]	V' [km/h]	k_{res}
Toyota Echo	56.5	1138	140.1	3.8	9.3	137.3	55.9	2.9	8.3	0.147
	56.3	1136	138.9	2.6	7.7	135.4	55.6	3.5	9.0	0.160
	48.5	1142	103.6	3.9	9.4	101.2	48.0	2.4	7.0	0.144
	47.8	1158	102.1	2.8	7.9	99.9	47.3	2.2	7.1	0.148
	40.3	1147	71.9	3.1	8.4	70.1	39.7	1.8	6.6	0.165
	40.5	1099	69.5	3.7	9.3	67.8	39.9	1.7	6.7	0.167
Honda Accord	55.6	1597	190.6	7.4	11.0	181.3	54.2	9.3	12.3	0.221
	55.7	1589	190.2	6.8	10.5	183.2	54.7	7.0	10.7	0.192
	48.1	1520	135.7	8.3	11.9	134.3	47.9	1.4	4.8	0.101
	47.9	1555	137.6	5.8	9.8	135.6	47.6	2.1	5.8	0.120
	40.2	1556	97.0	5.8	9.8	96.2	40.0	0.8	4.1	0.103
	40.2	1500	93.5	7.0	11.0	93.3	40.2	0.2	1.8	0.046
Ford Escape	56.3	1794	219.4	6.8	9.9	216.8	56.0	2.6	6.1	0.108
	56.3	1740	212.8	6.4	9.8	209.2	55.8	3.6	7.5	0.133
	48.2	1781	159.6	7.1	10.2	158.3	48.0	1.3	4.3	0.090
	47.8	1796	158.3	6.6	9.8	157.1	47.6	1.2	4.5	0.094
	40.0	1797	110.9	5.8	9.1	109.4	39.7	1.5	4.6	0.115
	40.1	1733	107.5	6.5	9.9	106.5	39.9	1.0	4.0	0.099

5. The simplified method

In the simplified method, the force causing a vehicle deformation is assumed to be proportional to the deformation depth. The deformation work ED is defined with the use of the stiffness coefficient k^*, which is considered in relation to the deformation area [3, 9, 10, 11]:

$$E_D = 0.5 \cdot w_D \cdot h \cdot C^2 \cdot k^* \quad [J] \qquad (13)$$

where: w_D, h – averaged deformation width and height, respectively [m]; C – deformation depth [m]; k^* – unit stiffness coefficient [N/(m·m²)].

At an assumption that $E_k = E_D$, the vehicle velocity at the beginning of the phase of collision with a rigid barrier may be determined as follows, based on (13):

$$V = \sqrt{\frac{2E_D}{m}} = \sqrt{\frac{w_D \cdot h \cdot k^*}{m}} \cdot C \qquad (14)$$

If the dimensions w_D and h are assumed to depend on the deformation depth to a small extent only, then the relation between V and C as defined by (14) may be considered linear. For the relation (14) to be used in practice, the dimensions of vehicle deformation (w_D, h, and C) and the value of coefficient k^* should be known. Example values of the coefficient k^* have been given in publications [3, 8, 9, 10, 11].

Fig. 8 shows the contours of the front part of the vehicles under consideration, which were used for determining the averaged height of the deformed zone. The drawing presented has been based on the photographic documentation of the cars involved, included in the test reports [26]. The height of the deformed zone at the distance of C^* was denoted in the analysis by h_c (Table 6). The averaged deformation height h was calculated in a similar way to $C_{śr}$ (equation (1)). It is worth stressing here that the method of determining the averaged deformation height h is no less troublesome than that used to determine the deformation depth $C_{śr}$ described previously. Moreover, the descriptions of the simplified method [10, 11] do not provide information about the method of calculation of the averaged deformation width and height (w_D, h).
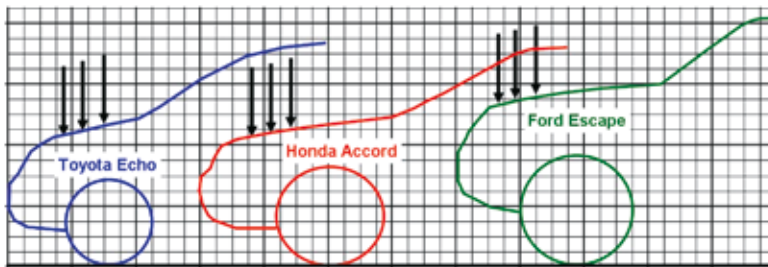
Fig. 8. Contours of the front part of the vehicles under consideration (the arrows indicate the range of deformation at impact velocities of 40 km/h, 48 km/h, and 56 km/h)

Table 6 shows a summary of the data used to calculate the impact velocities according to (14) for the three cars under analysis. It was assumed at the calculations that $C = C^*$ and that the averaged deformation width w_D was equal to vehicle width, i.e. $w_D = S$ (the reasons for making the latter assumption have been explained previously in this paper, beneath Table 2). Due to unavailability of the values of coefficient k^* for the cars under analysis, three values of this coefficient were assumed, i.e. $10 \cdot 10^5$ N/(m·m²), $15 \cdot 10^5$ N/(m·m²), and $20 \cdot 10^5$ N/(m·m²), based on [11]. Results of calculations of the impact velocities have been presented in Fig. 9. In spite of a wide range of the k^* coefficient values adopted for the calculations, the impact velocity values calculated for the Honda Accord and Ford Escape cars for the 40 km/h test velocity option were much lower than the actual test velocity.

Table 6. Results of calculations of the averaged deformation height h and the required values of coefficient $k*$

Velocity [km/h]	Toyota Echo			Honda Accord			Ford Escape		
	40	48	56	40	48	56	40	48	56
h_c [m]	0.61	0.65	0.68	0.59	0.61	0.64	0.67	0.72	0.77
h [m]	0.489	0.519	0.545	0.464	0.518	0.538	0.503	0.558	0.597
k_w* [N/(m·m²)·10⁵]	13.9	11.2	12.5	23.9	15.7	12.3	30.5	22.0	16.6
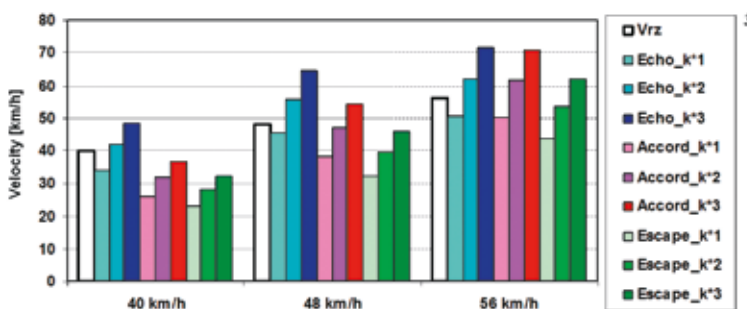
Fig. 9. Results of calculations of the impact velocities, obtained with the use of data of Tables 2 and 6

The bottom row of Table 6 shows the required values of coefficient $k*$ (denoted by k_w*). It only happened in the case of the Toyota Echo car that the k_w* values depended to a relatively small extent on the impact velocity, i.e. these values fell within a range of $k_w* = (11.2–13.9)\cdot10^5$ N/(m·m²) (in publication [9], this range has been specified as $(11.9–15.5)\cdot10^5$ N/(m·m²)). For the Honda Accord and Ford Escape cars, the k_w* values were found to largely depend on the impact velocity, which significantly reduces the usability of this energy method. Similar dependencies of the $k*$ values on the impact velocity, determined for other motor cars, have been given in publication [8].

6. The Campbell method

In the Campbell method, a linear relation between the velocity V of impact against a barrier and the depth C of permanent deformation of the vehicle body has been assumed [2, 10, 11, 20, 24]:

$$V = b_0 + b_1 \cdot C \qquad (15)$$

where: b_0 – the limiting velocity at which permanent deformation of the vehicle body begins to occur; b_1 – slope of the straight line in the graph $V = f(C)$.

---

[3] The symbol Vrz, wherever used in this paper, has the meaning of the actual vehicle impact velocity. *Translator's note.*

The b_0 and b_1 coefficient values for a few categories of passenger cars manufactured in 1970s have been given in Table 7. Fig. 10 shows relations between the velocity of impact against a barrier and the bodywork deformations $C*$ and $C_{śr}$ for the cars covered in Table 3. The straight lines in the graphs represent equation (15) for the b_0 and b_1 coefficient values taken from Table 7. In the graphs plotted for cars manufactured in the period 1974–1989 (Fig. 10a), many points are clustered around the straight lines, which confirms that the b_0 and b_1 coefficient values taken from Table 7 adequately represent the relations between the bodywork deformation and the velocity of impact against a barrier for many cars. For the cars manufactured in 1994–2013 (Fig. 10b), almost all points in the graphs are situated above the straight lines, i.e. the actual velocity was either higher or even much higher than the velocity calculated with the use of the b_0 and b_1 coefficient values taken from Table 7.

Table 7. The b_0 and b_1 coefficient values for General Motors cars [2]

Car model years	Car category	Mass [kg]	b_0 [km/h]	b_1 [(km/h)/m]
1971–1974	Small (subcompact)	1130	4.8	85.5
1971–1974	Compact	1540		
1973–1974	Intermediate	1810	12.1	55.7
1973–1974	Large (full size)	2040		

Attention is attracted by the wide range of deformations of cars at a specific impact velocity value. This significantly reduces the possibility of approximation of results obtained for a specific car category by a single linear function. The car similarity criteria must be

Fig. 10. Relations between the car body deformation and the velocity of a car impact against a barrier:
a) car model years 1974–1989 (n = 236); b) car model years 1994–2013 (n = 240)
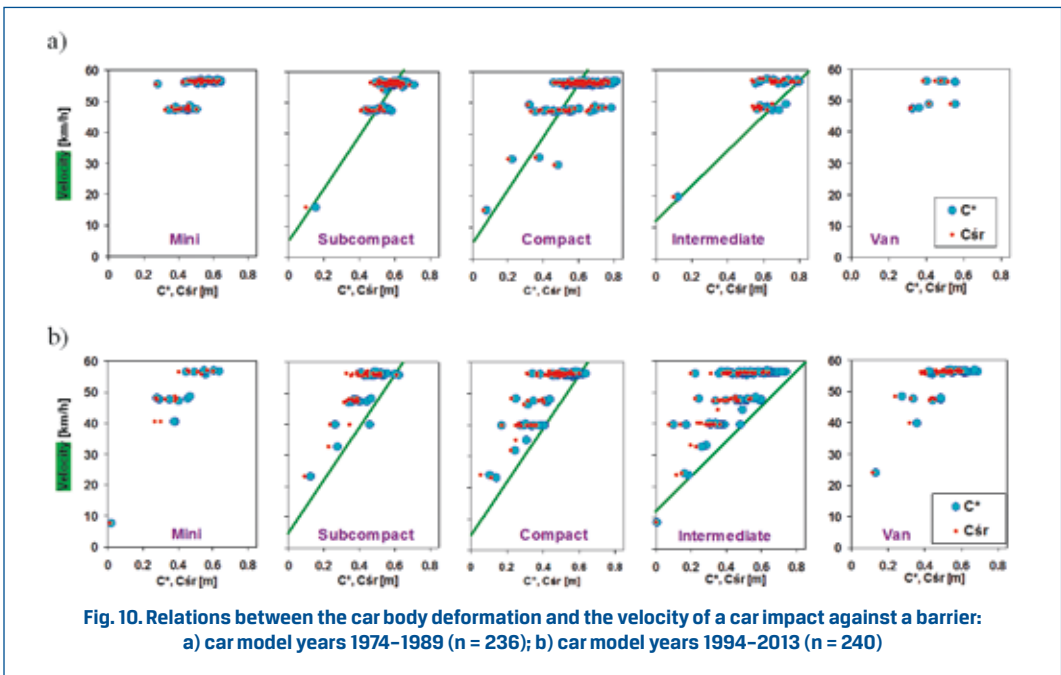
more precise, where not only the vehicle mass and dimensions (cf. Table 3) but also the bodywork construction, engine cubic capacity and position (transverse or longitudinal), front overhang, tyre size, etc. should be taken into account.

The application of the b_0 and b_1 coefficient values taken from Table 7 to the cars covered in Table 1 did not produce satisfactory results, either. Based on the vehicle mass, the values of these coefficients were b_0 = 4.8 km/h and b_1 = 85.3 (km/h)/m for the Toyota Echo and Honda Accord and b_0 = 12.1 km/h and b_1 = 55.7 (km/h)/m for the Ford Escape. The impact velocity values calculated according to (15) have been presented in Fig. 11. They show that the calculated impact velocity figures were usually much lower than the actual values:

– for the Toyota Echo, they made 73.4–92.3% of the actual value;

– for the Honda Accord, they made 69.8–95.4% of the actual value;

– for the Ford Escape, they made 63.4–71.3% of the actual value.
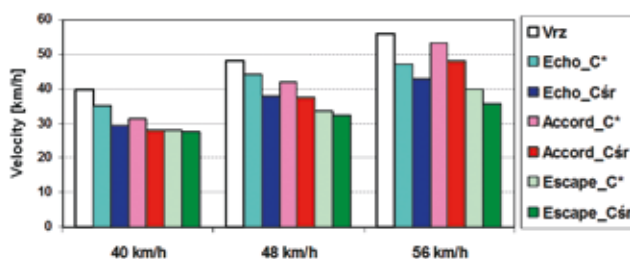
Fig. 11. Results of calculations of the impact velocities, obtained with the use of the b0 and b1 coefficient values taken from Table 7

Thus, it was confirmed that the use of coefficients b_0 and b_1 prepared for other motor vehicle constructions might be a source of errors at the reconstruction of accidents. Therefore, the b_0 and b_1 coefficient values were specially calculated for the three cars being analysed within this work. The calculations were made with using the results of deformation measurements carried out at the specific impact velocities (i.e. the data given in Fig. 3 and Table 2). The graphs representing the function $V = f(C)$ for the cars under analysis have been presented in Fig. 12, with trend lines having been plotted through the points that define the bodywork deformations C^* and $C_{śr}$. The trend lines differ from those presented in Fig. 7 because they have been plotted for plastic deformations (C) rather than dynamic deformations (D). Consistently with the assumptions made for the Campbell model, the trend lines intersect the vertical axis of the graph at the b_0 limiting velocity. For the Honda Accord, the b_0 value is about 23 km/h; for the Ford Escape, we have b_0 ranging from 9 km/h to 19 km/h.

The b_0 values being so high seem to be questionable, the more so that the limiting velocity values previously obtained from the stiffness characteristics were considerably lower (V_0 in Table 5). However, there is a lack of current data about present-day cars, capable to confirm the correctness of the V_0 values obtained as presented in Section 4. In publication

[16] of 1986, a proposal was made that the value of $V_0 = b_0$ should be assumed as not less than 8 km/h (5 mph). According to publication [17] of 1998, the deformation of a Ford Escort car having hit a barrier with a velocity of 13 km/h was 0.05 m. The NHTSA database [26] offers results of only about a dozen crash tests carried out where the velocity of a car impact against a rigid barrier was below 40 km/h; those data have been included in the data represented in Fig. 10. Regardless of the vehicle mass, the vehicle deformations (C^*) at impact velocities of 23 km/h and 32 km/h fell within ranges of 0.10–0.19 m and 0.24–0.32 m, respectively. A small plastic deformation (0.01–0.02 m) was reported to occur at as low an impact velocity as about 7 km/h. In consideration of all the above, an assumption was made for all the three cars that V_0 = 6 km/h and trend lines were plotted in the $V = f(C)$ graphs for such an assumption. The calculation results have been shown in Fig. 12b; the b_0 and b_1 coefficient values determined on these grounds have been brought together in Table 8.
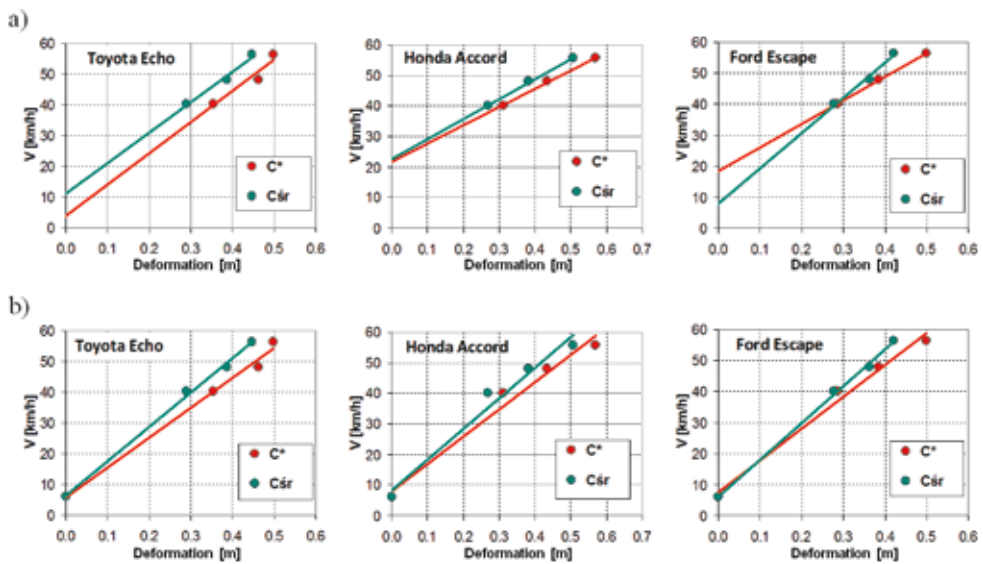
Fig. 12. Relations between the vehicle impact velocity and the plastic deformation:
a) direct linear approximation of the measurement results;
b) approximation at an assumption that b_0 = 6 km/h

Table 8. The b_0 and b_1 coefficient values for the Toyota Echo, Honda Accord, and Ford Escape cars

Coefficient	Toyota Echo		Honda Accord		Ford Escape	
	$C = C^*$	$C = C_{śr}$	$C = C^*$	$C = C_{śr}$	$C = C^*$	$C = C_{śr}$
b_0 [km/h]	5.9	6.4	8.2	8.5	7.60	6.10
b_1 [(km/h)/m]	97.0	111.8	89.1	100.1	102.7	118.5
D_0 [m]	0.061	0.057	0.092	0.085	0.074	0.051

The impact velocity values calculated according to (15) for the b_0 and b_1 coefficients determined as described above have been presented in Fig. 13. The calculated figures were now quite close to the actual values:

– for the Toyota Echo, they made 95.5–105.4% of the actual value;

– for the Honda Accord, they made 88.4–106.3% of the actual value;

– for the Ford Escape, they made 92.3–104.5% of the actual value.

Obviously, should the b_0 and b_1 coefficient values be determined from Fig. 12a) then the differences between the calculated and actual impact velocity values, within the range 40–56 km/h, would be even smaller than those specified above. However, the use of the model parameters thus prepared might result in worsening in the calculation results within the range of lower velocities.
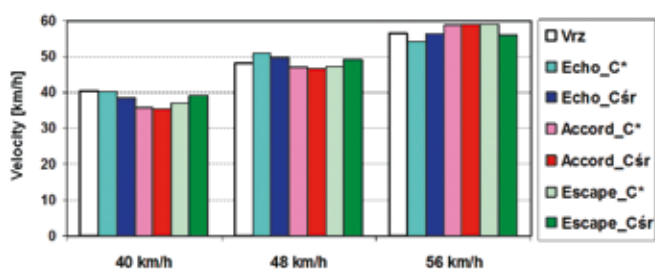
Fig. 13. Results of calculations of the impact velocities, obtained with the use of the b_0 and b_1 coefficient values taken from Table 8

Based on (15), the following equation may be formulated:

$$V = b_1 \cdot C + b_0 = b_1 \cdot (C + D_0) \qquad (16)$$

and the elastic deformation D_0 at the beginning of the vehicle body crushing process may be calculated:

$$D_0 = \frac{b_0}{b_1} \qquad (17)$$

The D_0 values thus calculated (Table 8) are close to the values determined from the stiffness characteristics (Table 4); this can be considered a confirmation of the correctness of the assumptions adopted for the calculations.

7. The McHenry method

In the McHenry method, a linear relation between the unit deformation force f_D, considered in relation to the overall vehicle body width, and the plastic deformation of the vehicle body has been assumed [6, 7, 11, 20, 24]:

$$f_D = A + B \cdot C_{pl} \tag{18}$$

where: A – unit force limit [N/m], such that when it is exceeded then plastic deformation begins to take place; B – slope of the straight line in the graph $f_D = f(C)$ [(N/m)/m]; C_{pl} – plastic deformation of the car body [m].
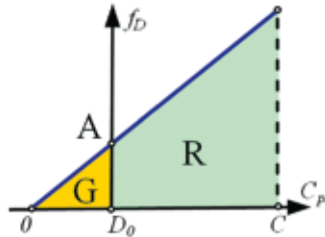
Fig. 14. Linear model of the bodywork stiffness, adopted by McHenry: D_0 – elastic deformation of the car body

Based on (17), the total energy of the plastic and elastic deformation of the car body is described by the following equation:

$$E_D = w_D \cdot \int_0^C f_D dC_{pl} = w_D \cdot (G + R) = w_D \cdot \left(\frac{A^2}{2 \cdot B} + A \cdot C + \frac{B \cdot C^2}{2} \right) \tag{19}$$

where: w_D – deformation width; G – unit energy of elastic deformation; R – unit energy of plastic deformation.

The A and B parameter values depend on the properties of the front crumple zone of the vehicle involved. The A and B parameter values, averaged for specific vehicle categories, have been given in Table 9 [11]. Relations between the actual velocity V_{rz} and the velocity V_D calculated from (9) and (19) with the use of results of crash tests of the cars covered in Table 3 have been presented in Fig. 15. The calculations were carried out with taking into account the deformations C^* and $C_{śr}$.

Table 9. The A and B coefficient values used in the CRASH3 program (*Computer Reconstruction of Accident Speeds on the Highway*)

Category	Wheelbase [m]	Length [m]	Width [m]	Mass [kg]	A [kN/m]	B [kN/m²]
Mini (M)	2.05...2.40	4.05	1.54	1000	52.9	320
Subcompact (S)	2.40...2.58	4.44	1.70	1386	45.4	300
Compact (C)	2.58...2.80	4.98	1.84	1610	55.5	390
Intermediate (I)	2.80...2.98	5.40	1.95	1928	62.3	230
Van (V)	2.76...3.30	4.66	2.00	1952	67.1	870
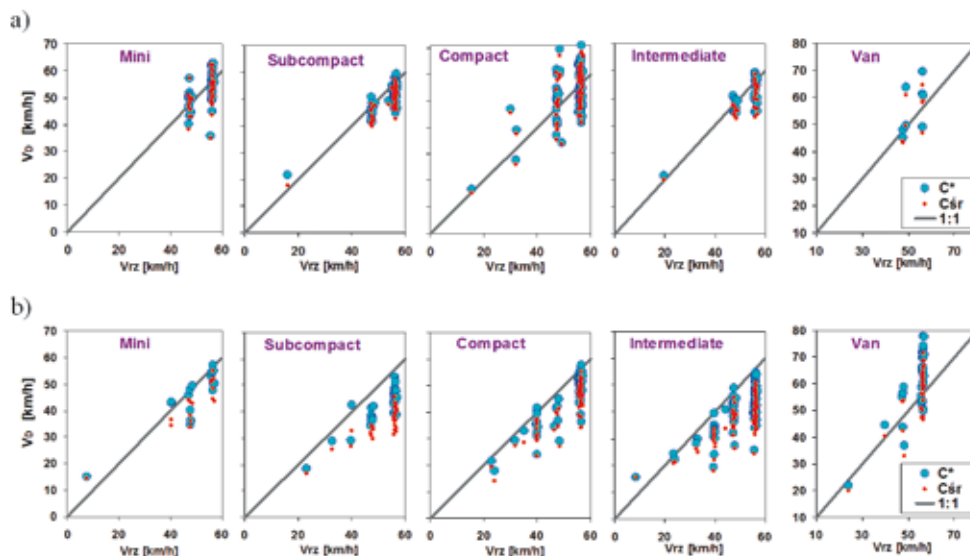
Fig. 15. Relations between the actual impact velocity and the impact velocity calculated from equations (9) and (19), with the A and *B* coefficient values taken from Table 9: a) car model years 1974–1989 (n = 236); b) car model years 1994–2013 (n = 240)

For a significant number of motor cars manufactured in the years 1974–1989, the calculated and actual impact velocity values (V_D and V_{rz}, respectively) are close to each other. For the cars manufactured in the years 1994–2013, the impact velocity calculation results V_D are markedly lower than the corresponding actual velocity values V_{rz}. This is a direct consequence of the previous findings that the deformation values recorded for present-day cars are lower than those observed in the cars made in 1974 to 1989 (cf. Fig. 4).

If the A and B coefficients are to be selected from Table 9 for the three cars under analysis, the cars must be classified under appropriate categories. This is difficult to be done, if the vehicle mass and dimensions are the only criteria of selection; therefore, each of the cars was classified under two categories. The results of calculations of the impact velocities for the A and B coefficients taken from Table 9, obtained with taking into account the C^* deformation values specified in Table 2, have been presented in Fig. 16. The calculated velocity values were lower than the corresponding values of the actual velocities. The differences were as follows:

– Toyota Echo (mass 1140 kg), 2–11% (mini) and 7–16% (subcompact);
– Honda Accord (mass 1550 kg), 5–19% (subcompact) and 15–28% (compact);
– Ford Escape (mass 1770 kg), 30–34% (compact) and 22–29% (intermediate).
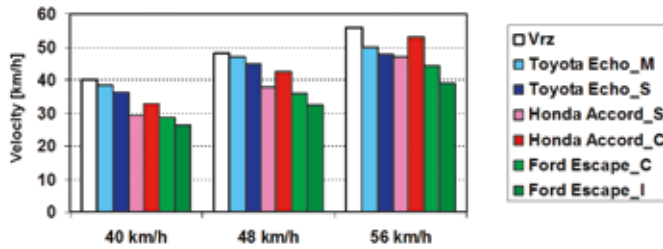
Fig. 16. Results of calculations of the impact velocities, obtained with the use of the A and B coefficient values taken from Table 9 (letters M, S, C, and I indicate the vehicle category, according to Table 3)

The examples of the calculation results that have been presented in Figs. 15b and 16 confirm that the use of the A and B coefficients prepared for the older vehicle constructions may be a source of considerable errors at the calculation of the impact velocity. Should the $C_{śr}$ values be used instead of C^*, the calculated velocity figures would be even lower, because $C_{śr} < C^*$ (Table 2). For the appropriate values of the A and B coefficients to be determined for the cars under analysis, the bodywork stiffness curves were averaged and divided into two parts (cf. Figs. 14 and 17), with the first one covering the elastic deformation range (up to the value of D_0). The force values were divided by the deformation width ($w_D = S$) for unit bodywork stiffness curves to be obtained. The curves were then approximated by linear functions (with the end sections of the curves being ignored). Thus, three linear equations were obtained for each car, corresponding to the velocities of 40 km/h, 48 km/h, and 56 km/h. The average values of the coefficients of these equations were adopted as the A and B coefficient values in the McHenry model. These values have been brought together in Table 10.

Table 10. Parameters of the McHenry model, determined from the bodywork stiffness curves

Vehicle	Toyota Echo			Honda Accord			Ford Escape		
Velocity [km/h]	40	48	56	40	48	56	40	48	56
A [kN/m]	45.5	40.1	39.9	73.9	80.6	87.7	73.6	81.1	81.9
$A_{śr}$ [kN/m]		41.8			80.7			78.9	
B [kN/m²]	355.1	417.1	423.5	260.5	240.7	249.8	719.7	701.7	729.6
$B_{śr}$ [kN/m²]		399			250			717	
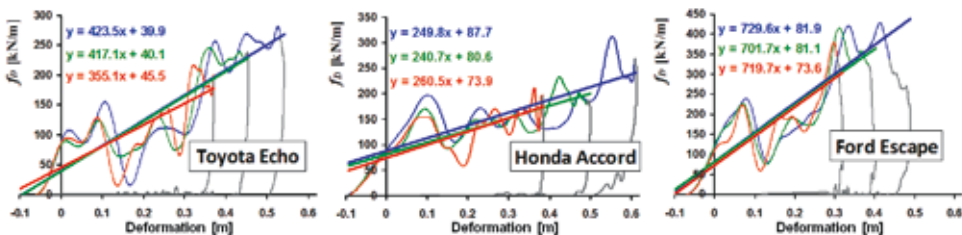
Fig. 17. Linear approximation of the unit bodywork stiffness curves
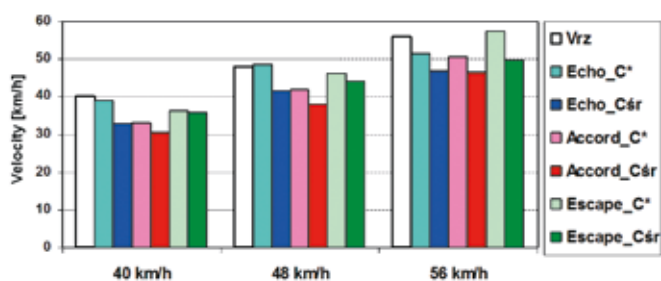
Fig. 18. Results of calculations of the impact velocities, obtained with the use of the $A_{śr}$ and $B_{śr}$ coefficient values

Now, the impact velocities were calculated from (9) and (19) for the $A_{śr}$ and $B_{śr}$ coefficient values having been determined as described above and the following relations between the calculated and actual impact velocity values were obtained (Fig. 18):

- for the Toyota Echo, the calculated figures made 81.4–100.7% of the actual value;
- for the Honda Accord, the calculated figures made 75.4–91.0% of the actual value;
- for the Ford Escape, the calculated figures made 88.1–101.9% of the actual value.

In comparison with the results produced by the Campbell method (Fig. 13), these results of calculations of the impact velocities were more different from the actual velocity values. The biggest differences occurred in the case of the Honda Accord, where every calculated value of the impact velocity was lower by 9–24% than the corresponding actual value.

8. Results of conversion of parameters of the Campbell and McHenry models

The values of parameters of the Campbell and Mc Henry models were determined from the same crash tests, but different quantities, measured during tests of the cars under analysis, were now taken as a basis. Since both the energy models are applied to the same vehicle body deformation process, the relations between parameters of these models may be represented by the following equations [5, 11, 20, 24]:

$$b_0 = A \cdot \sqrt{\frac{w_D}{B \cdot m}}, \; b_1 = \sqrt{\frac{B \cdot w_D}{m}} \tag{20}$$

$$A = \frac{m \cdot b_0 \cdot b_1}{w_D}, \; B = \frac{m \cdot b_1^2}{w_D} \tag{21}$$

The model parameter values thus calculated have been brought together in Tables 11 and 12. The A and B coefficient values were calculated with taking into account the values of parameters b_0 and b_1, which were previously determined with assuming $C = C^*$ and $C = C_{śr}$ (cf. Table 8). A graphic illustration of applying the parameters taken from Tables 8, 10, 11, and 12 has been presented in Fig. 19.

Table 11. The b_0, b_1, and D_0 parameter values calculated from (20) and (17)

Parameter	Toyota Echo	Honda Accord	Ford Escape
b_0 [km/h]	9.1	19.7	10.5
b_1 [(km/h)/m]	86.9	61.0	95.8
D_0 [m]	0.105	0.322	0.110

Table 12. The A and B parameter values calculated from (21)

Parameter	Toyota Echo		Honda Accord		Ford Escape	
	$C = C^*$	$C = C_{śr}$	$C = C^*$	$C = C_{śr}$	$C = C^*$	$C = C_{śr}$
A [kN/m]	30.1	38.0	49.3	57.3	61.0	56.5
B [kN/m²]	497	661	534	674	825	1098

In the case of Toyota Echo and Ford Escape, the lines denoted by (A, B) and (C^*) are similar to each other, which confirms that both methods offered similar results. The line denoted by ($C_{śr}$) is markedly different, which results from a relation $C_{śr} < C^*$. For Honda Accord, much bigger differences were obtained. It should be noted, however, that the Campbell model parameter values given in Table 11 for Honda Accord, calculated for the $A_{śr}$ and $B_{śr}$ values given in Table 10, are quite unlikely to occur in practice (b_0 = 19.7 km/h, D_0 = 0.32 m).

Fig. 19. Results of applying a conversion of coefficients of the Campbell and Mc Henry models: a) relation between the impact velocity and the plastic deformation; b) approximation of unit bodywork stiffness curves by linear functions (A, B – lines plotted on the grounds of the stiffness characteristics; C^* and $C_{śr}$ – lines plotted on the grounds of the plastic deformation of the cars)
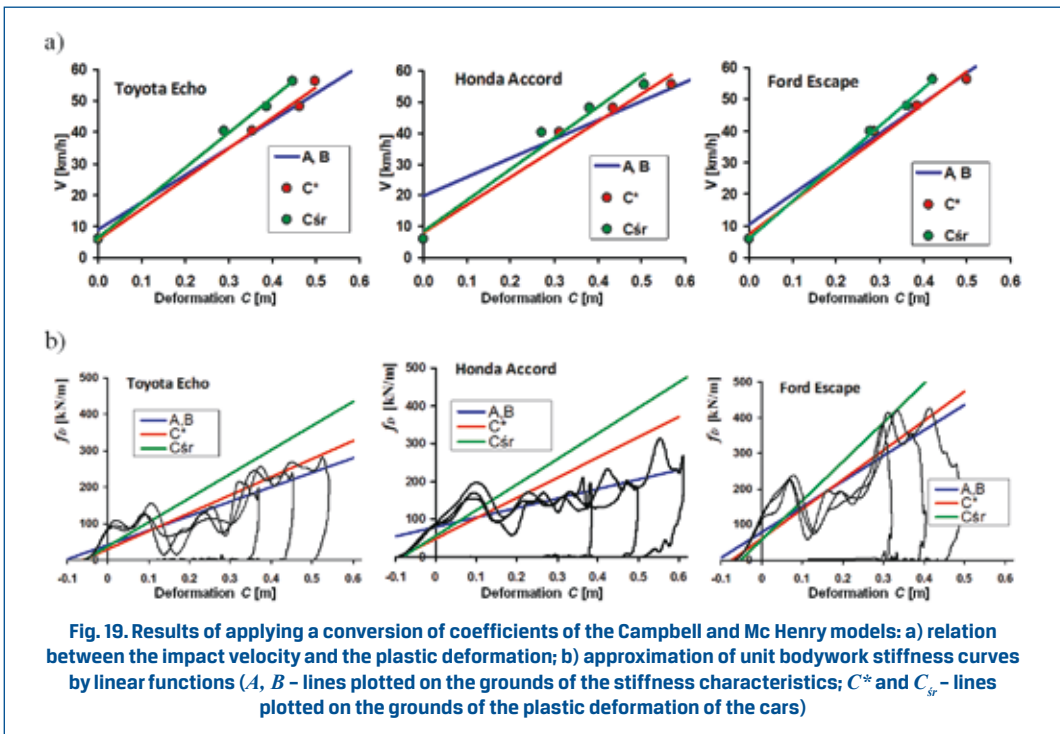
This example of calculations confirms that the impact velocity calculation results obtained for some vehicles with the use of linear energy models may be burdened with significant errors.

9. Conclusions

1. The application of energy methods is limited by the availability of linear model parameters (k^*, b_0, b_1, A, B) for present-day cars. The frontal impact of a motor car against a rigid barrier is the simplest collision type from the process analysis point of view; nevertheless, the determining of parameters of the analysed energy models for the three motor cars under consideration turned out to be quite a difficult task and the impact velocity calculation results obtained for the parameter values having been determined were satisfactory for not all of the cars.

2. The measurements of vehicle deformation are quite troublesome; on the other hand, the measurement results may considerably affect the impact velocity value having been calculated. Therefore, it is essential that the method of defining the measured dimensions of the deformed zone (C, w_D, h) should be precisely specified. This is particularly important at the analysis of deformation of present-day cars, where the crumple zones are more rigid than they were in the older designs of integral car bodies (cf. Fig. 4). In the case of cars where a change in the impact velocity does not result in a considerable change in the bodywork deformation, the results of calculations based on linear models may be burdened with significant errors.

3. The simplified method, based on the unit stiffness coefficient k^*, proved to be effective only for the Toyota Echo car. In the case of Honda Accord and Ford Escape, the k^* coefficient value was found to be strongly dependent on the impact velocity, which practically precludes the use of this method if an assumption is to be made that $k^* = $ const.

4. The determining of model parameters for the McHenry method was based on an analysis of the vehicle bodywork stiffness curve, which usually is strongly non-linear, and this reduces the correctness of describing it with the use of linear models. The determining of the A and B coefficient values for the McHenry method is labour-consuming, but the relations between the impact velocity and the bodywork deformation may be estimated on the grounds of only one crash test (i.e. only one car is destroyed), which is unquestionably a good point of this method.

5. The best results of impact velocity calculations were obtained when the Campbell method was used. However, several crash tests with various impact velocity values must be taken into account (i.e. must have been actually carried out) for the b_0 and b_1 coefficient values to be adequately determined. The selection of parameter values for the Campbell model was difficult because of the lack of reliable data about the deformation of present-day cars at low impact velocity values. This problem can be solved by specifying model parameters for a limited deformation range.

6. The research results presented here provide grounds for a statement that the linear models poorly represent the properties of the front crumple zone of present-day cars. Even if the values of parameters of the energy models have been determined for specific vehicles in result of an in-depth analysis of data obtained from actual tests of the vehicles, the model analysis results may be incorrect. In the examples presented here, the calculated impact velocity values differed sometimes from the actual figures by as much as 20%. Even worse results were obtained when the values adopted for the energy model parameters had been determined for vehicles of different construction (the differences were then around 30%).

7. In consideration of the fact that the results of reconstruction of road accidents are used at legal actions and have a social aspect as well, the parameters of energy models should be prepared in a way making it possible to determine the uncertainty of the calculation result obtained. Such a need is also highlighted by other authors, e.g. in publications [4, 23]. Possibilities of this kind are offered by the test results gathered in the NHTSA database [26], where information about side collisions, including collisions with a pole, is available. However, the results presented in Fig. 10 show that the possibility of preparing the parameters of linear energy models for a specific vehicle category may be very limited because of significant scatter of the results caused by the diversity of characteristics of the car crumple zones, even if the cars are similar to each other.

References

[1]   Brach, R. M.; Brach, R. M.: *Vehicle Accident Analysis and Reconstruction Methods*. SAE International, USA, 2011.

[2]   Campbell, K. L.: *Energy Basis for Collision Severity*. SAE Paper 740565, 1974.

[3]   Diupero, T.; Górny, A.; Wolski, E.: *Ustalanie prędkości zderzenia w oparciu o zakres uszkodzeń samochodu* (*Determining the impact velocity based on the scope of vehicle damage*). Rzeczoznawca Samochodowy 8/2000.

[4]   Jiang, T.; Grzebieta, R. H.; Rechnitzer, G.; Richardson, S.; Zhao, X. L.: *Review of Car Frontal Stiffness Equations for Estimating Vehicle Impact Velocities*. The 18th International Technical Conference on the Enhanced Safety of Vehicles Conference (ESV), Nagoya, 2003.

[5]   Jankowski, P.; Gidlewski, M.; Jemioł, L.: *Comparative Study of Vehicle Absorbed Energy Determination for Road Accident Reconstruction*. The 16th EVU Conference "Uncertainty in the Reconstruction of Road Accidents", Kraków 2007.

[6]   Mchenry, R. R.; Mchenry, B. G.: *Effects of Restitution in the Application of Crush Coefficients.* SAE Paper 970960, 1997.

[7]   Mchenry, R. R.; Mchenry, B. G.: *A Revised Damage Analysis Procedure for the CRASH Computer Program*. SAE Paper 861894, 1986.

[8]   Owsiański, R.: *Rastry energetyczne samochodów osobowych dla zderzeń czołowych* (*Passenger car energy rasters for frontal collisions*). Paragraf na Drodze No. 9/2007.

[9]   Owsiański, R.: *Szacowanie energii deformacji nadwozi kompaktowych samochodów osobowych* (*Estimation of the bodywork deformation energy of compact passenger cars*). Paragraf na Drodze No. 4/2007.

[10] Joint publication: *Wypadki drogowe. Vademecum biegłego sądowego* (*Road accidents. Forensic expert's vade mecum*). Issue 2, Institute of Forensic Research, Kraków 2006.

[11] Prochowski, L.; Unarski, J.; Wach, W.; Wicher, J.: *Podstawy rekonstrukcji wypadków drogowych* (*Fundamentals of the reconstruction of road accidents*). WKiŁ, Warszawa 2008.

[12] Prochowski, L.; Żuchowski, A.: *Rastry energetyczne wykorzystywane do opisu rozkładu energochłonności przedniej części nadwozia* (*Energy rasters used for describing the distribution of energy absorption in the front part of a vehicle bodywork*). The 4th Scientific and Educational Conference "Development of automotive engineering versus motor insurance", Radom, 2008.

[13] Prochowski, L.; Żuchowski, A.: *Rozkład energii pochłanianej podczas czołowego uderzenia samochodu w przeszkodę* (*Distribution of the energy absorbed during a frontal impact of a motor vehicle against an obstacle*). The 10th Conference "Road Accident Reconstruction Problems", Szczyrk 2006.

[14] Prochowski, L.; Żuchowski, A.: *Comparative Analysis of Frontal Zone of Deformation in Vehicles with Self-Supporting and Framed Bodies.* Journal of KONES Powertrain and Transport, Vol. 18, No. 4, Warszawa 2011.

[15] Prochowski, L.; Żuchowski, A.: *Właściwości nadwozia w zakresie pochłaniania energii podczas uderzenia samochodu w sztywną przeszkodę* (*Motor vehicle bodywork properties regarding the energy absorption during a vehicle impact against a rigid obstacle*). The 5th Scientific and Technical Conference "Safety Problems in Motor Vehicles", Kielce 2006.

[16] Strother, Ch. E.; Woolley, R. L.; James, M. B.; Warner, CH.: *Crush Energy in Accident Reconstruction.* SAE 860371, 1986.

[17] Steffan, H.; Geigl, B. C.; Moser, A.; Hoschopf, H.: *Comparison of 10 to 100 km/h Rigid Barrier Impacts.* The 16th International Technical Conference on the Enhanced Safety of Vehicles Conference (ESV), Windsor 1998.

[18] Vangi, D.: *Simplified Method for Evaluating Energy Loss in Vehicle Collisions.* Accident Analysis and Prevention, 41/2009.

[19] Varat, M. S.; Husher, S. E.: *Crash Pulse Modelling for Vehicle Safety Research.* The 18th International Technical Conference on the Enhanced Safety of Vehicles Conference (ESV), Nagoya, 2003.

[20] Wach, W.: *Amerykańskie standardy analizy zderzeń pojazdów* (*American standards of the analysis of vehicle collisions*). The 8th Conference "Road Accident Reconstruction Problems", Institute of Forensic Research, Kraków 2002.

[21] Wach, W.: *Analiza deformacji samochodu według standardu CRASH3. Część 1: Wprowadzenie* (*Analysis of motor vehicle deformation according to the CRASH3 standard. Part 1: Introduction*). Paragraf na Drodze No. 11/2003.

[22] Wach, W.: *Analiza deformacji samochodu według standardu CRASH3. Część 2: Pomiar głębokości odkształcenia* (*Analysis of motor vehicle deformation according to the CRASH3 standard. Part 2: Measurement of deformation depth*). Paragraf na Drodze No. 12/2003.

[23] Wang, Q.; Gabler, H. C.: *Accuracy of Vehicle Frontal Stiffness Estimates for Crash Reconstruction.* The 20th International Technical Conference on the Enhanced Safety of Vehicles Conference (ESV), Lyon 2007.

[24] Wicher, J.: *Energetyczne metody analizy zderzeń samochodów* (*Energy methods of the analysis of motor vehicle collisions*). The 3rd Scientific and Educational Conference "Development of automotive engineering versus motor insurance", Radom 2006.

[25] Żuchowski, A.; Prochowski, L.: *Sztywność nadwozia – analiza sił działających na przeszkodę podczas zderzenia* (*Vehicle bodywork stiffness: analysis of the forces acting on the obstacle during a collision*). The 6th Scientific and Technical Conference "Safety Problems in Motor Vehicles", Kielce 2008.

[26] www.nhtsa.gov